

Enhanced Mass Transfer in Microbubble Driven Airlift Bioreactor for Microalgal Culture

Kezhen Ying^{1*}, Mahmood K. H. Al-Mashhadani¹, James O. Hanotu¹,
Daniel J. Gilmour², William B. Zimmerman¹

¹Department of Chemical and Biological Engineering, University of Sheffield,
Sheffield, UK

²Department of Molecular Biology and Biotechnology, University of Sheffield, Sheffield, UK
Email: *cpp09ky@sheffield.ac.uk

Received June 6, 2013; revised July 6, 2013; accepted July 13, 2013

Copyright © 2013 Kezhen Ying *et al.* This is an open access article distributed under the Creative Commons Attribution License, which permits unrestricted use, distribution, and reproduction in any medium, provided the original work is properly cited.

ABSTRACT

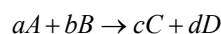
In this study, the effect of microfluidic microbubbles on overall gas-liquid mass transfer (CO₂ dissolution and O₂ removal) was investigated under five different flow rates. The effect of different liquid substrate on CO₂ mass transfer properties was also tested. The results showed that the K_La can be enhanced by either increasing the dosing flowrate or reducing the bubble size; however, increasing the flow rate to achieve a higher K_La would ultimately lower the CO₂ capture efficiency. In order to achieve both higher CO₂ mass transfer rate and capture efficiency, reducing bubble size (e.g. using microbubbles) has been proved more promising than increasing flow rate. Microbubble dosing with 5% CO₂ gas showed improved K_La by 30% - 100% across different flow rates, compared to fine-bubble dosing. In the real algal culture medium, there appears to be two distinct stages in terms of K_La , divided by the pH of 8.4.

Keywords: Microbubbles; K_La ; CO₂ Capture; Algal Culture

1. Introduction

The cultivation of microalgae has been studied and developed for more than 40 years [1]. Two of the major limiting factors for microalgal culture are light and CO₂ as they are the key participants for the “light reactions” and “dark reactions” in photosynthesis, respectively. Many researches have been carried out to study the impact of light on algal growth. Technical issues associated with light have been also well studied especially for photobioreactors, with various solutions (e.g. using an optimal mixing rate and light/dark ratio, combining artificial light with natural light, and increasing harvest frequency etc.) [2]. As regards to CO₂ supply, in most microalgal cultures, CO₂ is usually injected into the culture through bubbling CO₂ enriched air into porous diffusers, which promises a gas transfer efficiency of 13% - 20% [3]. Additional supply of CO₂ contributes many benefits to the culture. First of all, the supply of CO₂ can lead to enhanced algal metabolisms, and on the other hand, it can act as buffer solution to neutralize the increased pH caused by algal growth. Secondly, supply of CO₂ enhances the internal mixing of bioreactor, helping to

evenly distribute nutrients and the exposure time of algal cells to light. Furthermore, accumulation of O₂ in culture medium is toxic to microalgal cells and it is one of the major limiting factors for scale up of the bioreactor [4]. Introducing CO₂ into culture also helps to strip accumulated oxygen and hence prevents algal cells from toxicity [5]. According to the relationship between partial pressure and Gibbs free energy (Equation (1)), it is found that the increase in the partial pressure of reactants (e.g. CO₂) or the reduction of partial pressure in the products (e.g. O₂) results in the value of Gibbs free energy becoming negative. Hence the reaction becomes thermodynamically favourable and moves towards the formation of more products [6]. Such feature of performance is widely utilized for many bioprocesses to achieve a higher productivity [2,5]. Therefore by increasing the concentration of dissolved CO₂ whilst reducing the accumulated O₂ level can be considered as an approach towards improving productivity.



$$\Delta G = \Delta G^\circ + RT \ln \frac{[P_C]^c [P_D]^d}{[P_A]^a [P_B]^b} \quad (1)$$

*Corresponding author.

However, most existing CO₂ supply techniques are relatively inefficient. Due to low interfacial surface area between gas bubbles and culture medium, the gas-liquid mass transfer is poor, which associated with CO₂ loss to atmosphere [7]. Besides, additional CO₂ supply increases the operational cost, which can not be balanced eventually by the algal yields enhancement due to the low CO₂ mass transfer. Improving the CO₂ supply efficiency and consequently enhancing the algal productivity has become a major challenge over the years. Design of bioreactor with low energy cost and particularly high gas mass transfer for both CO₂ dissolution and O₂ removal is hence a major consideration for cost-competitive microalgae culture.

Due to the enhanced gas-liquid mass transfer efficiency and liquid circulation etc., airlift bioreactors (ALB) are increasingly employed for microalgae culture. Many researches have been carried out on the performance of different ALBs; however, these studies were carried out all based on conventional gas supply system. There are few studies on the effects of microbubbles on ALB performance, because normally the microbubble generation systems, for instance DAF, electro-flotation, electrostatic spraying, and mechanical agitation etc, were not profitable to be applied into most bio-processes due to their high energy cost [8-12]. Recently, an innovative microbubble generation system (fluidic oscillator) with lower power consumption has been invented by Zimmerman *et al.* [13,14] with the benefits of energy saving and improved efficiency. The detailed information on fluidic oscillator and its microbubble generation mechanism were described in previous studies [13-15]. This study aims to investigate the effect of microbubbles (generated by fluidic oscillator) on mass transfer under different aeration flow rates. In addition, the impact of different liquid substrate (e.g. NaHCO₃ medium and algae medium) on CO₂ mass transfer properties is investigated.

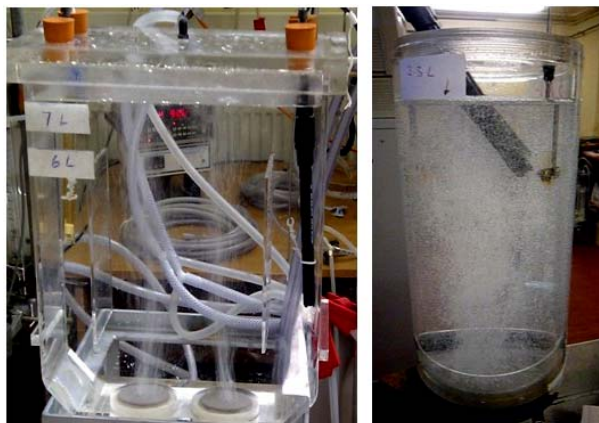
2. Materials and Methods

2.1. Materials

A 7L-airlift loop bioreactor based on classic ALB geometry designs [16], as shown in **Figure 1** (left), was used to study the mass transfer properties of microbubbles and fine-bubbles. Besides, a smaller version (3L) of ALB, based on the similar geometry design, was applied to study the impact of different liquids on mass transfer, shown in **Figure 1** (right).

2.2. Experimental Procedure

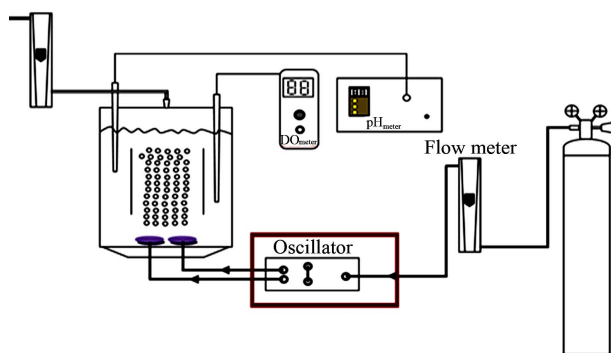
To study the mass transfer properties of microbubbles and fine-bubbles, the two inlet ports of diffusers at the bottom of bioreactor were connected to gas cylinder by PVC tubes, through a fluidic oscillator or a Y-junction.



The 7 L-airlift bioreactor is made of transparent acrylic material with the dimension of 26 cm × 10 cm × 30 cm. Inside the bioreactor, two ceramic diffusers ($d = 5$ cm, $h = 1$ cm), with the pore size of 20 microns, are fixed at the bottom. Two draught baffles are suspended 3.5 cm above these diffusers, dividing the middle chamber into 3 regions which work as risers and downcomers. A static liquid height of 15 cm was employed to give the volume of 7 L. There are several holes drilled on the lid to allow pH and DO probes insert into the reactor. The 3L- airlift bioreactor is also made of acrylic material, with the dimension of 285 mm in height and 124 mm in diameter. The air lift loop design consists of a ceramic diffuser (diameter of 78 mm and pore size of 20 microns) fixed at bottom and an internal draught tube (H: 170 mm, D: 95 mm) hanged 30 mm above the diffuser.

Figure 1. 7L (left) and 3L (right)—lab scale airlift loop bioreactors (ALB).

The detailed connections for main experiments (with oscillator) and control experiments (without oscillator) are illustrated in **Figure 2**. A pH and DO probe (Mettler Toledo, UK) were inserted into the bioreactor via the holes on the lid. These holes were blocked by rubber bungs to prevent gas leakage. The outlet nozzle on the lid was connected to a flow meter to measure the outlet flowrate which is equal to the real inlet flowrate. For each set of experiment, 7L distilled water with the temperature $25^{\circ}\text{C} \pm 1^{\circ}\text{C}$ were employed. Mixture gas containing 5% CO₂ and 95% N₂ was injected into bioreactor under certain flow rate. Five different flow rates were tested. The flow rate was measured by a flow meter which was connected to the outlet port of the bioreactor. The changes in pH and DO were monitored by pH meter and DO meter respectively. Data was recorded every 30 seconds until pH and DO readings were stable. The effect of different liquids on mass transfer was studied in the 3L-ALB with the same setup as shown in **Figure 2**. The mass transfer for CO₂ dissolution was tested in the distilled water containing certain concentration of NaHCO₃ and also in the real algal culture medium (containing algae). 7 different concentrations of NaHCO₃ were tested. The algae (*Dunaliella salina*) used in this study was 7 days old. During the mass transfer test, 5% CO₂ and 95% N₂ was injected into *D. Salina* culture under a fixed dosing flow rate (0.7L/min), with DO and pH recorded every 30 seconds. The dissolved CO₂ concentration was calculated based on Equation (2) (for water)



For microbubble dosing, the gas ejected from cylinder flowed into a fluidic oscillator, and was shot out from the two outlet terminals on oscillator. Here a flow rate of 80 L was required to drive the oscillator. Before such amount of gas injected into bioreactor, most of them were bled out via bleeding pipes with only less than 1% flowing into bioreactor, and the real inlet flow was measured by the flow meter at bioreactor output. For fine-bubble dosing, the area marked as red frame was placed with a Y-junction.

Figure 2. Connections for mass transfer test.

or Equation (3) (for NaHCO_3 medium and algal medium) [17]. $[\text{Na}^+]$ in Equation (3) particularly means the concentration of Na^+ obtained from NaHCO_3 . The method of mass transfer coefficient estimation was estimated as the slope of a semilog plot of $1/(1-E)$ versus T , which was explained in details in Chisti (1989) [16].

$$[\text{CO}_2] = \frac{(10^{-\text{pH}} - 10^{\text{pH}-14})10^{-2\text{pH}}}{10^{-6.381-\text{pH}} + 2 \times 10^{-16.758}} \text{ (mol/L)} \quad (2)$$

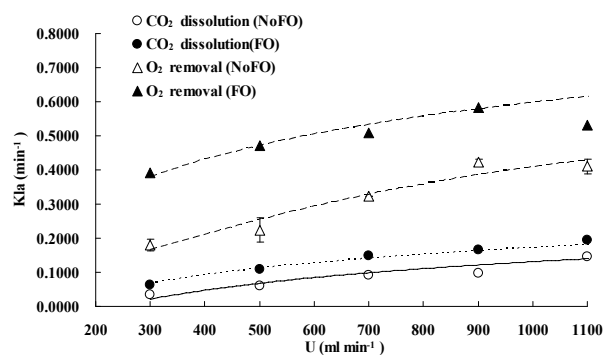
$$[\text{CO}_2] = \frac{(10^{-\text{pH}} - 10^{\text{pH}-14} + \Delta[\text{Na}^+])10^{-2\text{pH}}}{10^{-6.381-\text{pH}} + 2 \times 10^{-16.758}} \text{ (mol/L)} \quad (3)$$

3. Results and Discussions

3.1. Mass Transfer for Microbubble Driven and Fine-Bubble Driven Reactor

The effects of microbubble dosing on mass transfer for CO_2 dissolution and O_2 removal were examined by dosing 5% CO_2 mix-gas (balanced with 95% N_2) into bioreactor (containing 7L distilled water) under 5 different bubbling flow rates, along with the control experiment (without fluidic oscillator, fine bubble dosing). The mass transfer coefficient K_La for CO_2 dissolution and O_2 removal under each bubbling condition were plotted in Figure 3. From Figure 3, generally K_La for either CO_2 dissolution or O_2 stripping increases along with gas dosing flow rate. For K_La , K_L mainly depends on the gas-liquid properties (e.g. density, viscosity, diffusivity and temperature etc.), and therefore is usually considered as a constant for the fixed circumstance [16]. Chisti expressed the interfacial area “ a ” as a function of gas holdup (ϵ) and bubble diameter (d_B) [16], shown as:

$$a = \frac{6\epsilon}{d_B} \quad (4)$$



FO means “with fluidic oscillator”, representing microbubble (300 - 400 μm) dosing while NoFO stands for “without fluidic oscillator”, representing fine bubble (500 - 600 μm) dosing. Due to the lab limitations, the error bars shown in this figure was obtained from the duplication of fine bubble dosing under each flow rate (for O_2 removal, NoFO).

Figure 3. Mass transfer coefficients under different dosing conditions.

For the same bubbling system (either microbubble dosing or fine bubble dosing), the bubble size can be considered as the same for different gas dosing flowrates, while the gas holdup usually increases with the bubbling flowrate, therefore, K_La was enhanced by increasing the flowrate as the total interfacial area was amplified.

As regard the comparison of mass transfer coefficients (either for CO_2 dissolution or O_2 removal) between microbubble dosing (FO) and fine bubble dosing (NoFO), microbubbles had a higher mass transfer coefficient under each dosing flowrate. For CO_2 dissolution, the highest K_La under fine bubble dosing (0.14 min^{-1}) was achieved at dosing flow rate of $1.1 \text{ L}\cdot\text{min}^{-1}$, while almost the same K_La value (0.15 min^{-1}) was achieved by microbubble dosing at $0.7 \text{ L}\cdot\text{min}^{-1}$. Similarly, for O_2 removal the highest K_La (0.41 min^{-1}) was obtained at $1.1 \text{ L}\cdot\text{min}^{-1}$ by fine bubble dosing, which however can be achieved at only $0.3 \text{ L}\cdot\text{min}^{-1}$. The potential for energy saving, especially for large scale processes, is therefore straight forward to argue. For example, in order to dissolve more CO_2 and strip off O_2 accumulated in algal bioreactor, it would typically require dosing certain percentage of CO_2 mixture gas at a relatively high aeration rate to achieve a desired mass transfer coefficient. But actually, under very high flow rate, most of the gas is wasted. And an intensive agitation caused by high flow rate may damage the algal cells. However, by using oscillator (microbubble dosing) the desired K_La can be obtained even at relatively low flow rate. It considerably saves gas usage and also the electricity cost.

In conclusion, for the same bubble generation method (the changes in bubble sizes are considered to be negligible across a wide range of dosing flow rate), enhancing the gas dosing flowrate (which means enhancing the gas hold up for the same liquid volume) can increase the mass transfer coefficient. For the same bubbling flowrate,

reducing the bubble size can lead to an improvement on K_La as well. In another word, K_La can be enhanced by either increasing the dosing flowrate (to be more accurate, flowrate/liquid volume ratio) or reducing the bubble size.

3.2. The Improvement of K_La by Using Fluidic Oscillator

When injecting CO_2/N_2 mixture gas into water, CO_2 dissolution happens along with O_2 stripping. The improvements by using fluidic oscillator (microbubbles) on mass transfer for CO_2 dissolution and O_2 stripping can be simply quantified as the percentage increase in $K_{L(\text{CO}_2)}a$ and $K_{L(\text{O}_2)}a$, expressed in Equation (5) and Equation (6), respectively.

$$I_{K_{L(\text{CO}_2)}a} \% = \frac{K_{L(\text{CO}_2)}a_{\text{FO}} - K_{L(\text{CO}_2)}a_{\text{NoFO}}}{K_{L(\text{CO}_2)}a_{\text{NoFO}}} \quad (5)$$

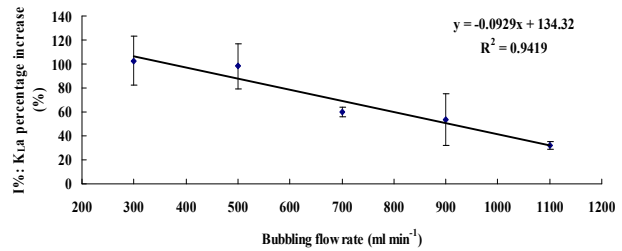
$$I_{K_{L(\text{O}_2)}a} \% = \frac{K_{L(\text{O}_2)}a_{\text{FO}} - K_{L(\text{O}_2)}a_{\text{NoFO}}}{K_{L(\text{O}_2)}a_{\text{NoFO}}} \quad (6)$$

Either Equation (5) or Equation (6) can be turned into Equation (7) which indicates the percentage increase in K_La by using microbubble dosing should be the same for either CO_2 dissolution or O_2 removal under a fixed bubbling flowrate. The percentage improvement of K_La is therefore determined by the percentage difference of the total interfacial areas for a certain dosing flow rate. Combining Equation (7) and Equation (4), the percentage increase in K_La is correlated to bubble diameter (d_B) and gas hold-up (ε), described by Equation (8).

$$I\% = I_{K_{L(\text{CO}_2)}a} \% = I_{K_{L(\text{O}_2)}a} \% = \frac{a_{\text{FO}} - a_{\text{NoFO}}}{a_{\text{NoFO}}} \quad (7)$$

$$I\% = \frac{\varepsilon_{\text{FO}} d_{B\text{NoFO}}}{\varepsilon_{\text{NoFO}} d_{B\text{FO}}} - 1 \quad (8)$$

From Equation (8), the efficiency of K_La improvement ($I\%$) therefore should be the same across different flow rates, assuming 1) the gas holdups are identical between microbubble dosing and fine bubble under the same flow rates, and 2) changing the flow rate dose not vary the average bubble size for either microbubbles or fine bubbles as long as the “bubble coalescence” does not happen. However, the experimental results are inconsistent with such speculation. **Figure 4** shows the K_La percentage increase. In general, microbubble dosing enhances the K_La by 30% - 100% over a wide flow rate range, while the efficiency of the improvement decreases when increasing the flow rate. It is speculated that the microbubble size increases with the flow rate. The fluidic oscillator provides a periodical oscillating pulse to neck-off the bubbles attached to the diffuser orifice when they are still



The value of $I\%$ under each flow rate was the average between the values calculated based on Equation (5) and Equation (6). The error bar represents the standard deviation between these two values.

Figure 4. Plots of K_La percentage increase versus dosing flow rate.

small. But for the same surface area of diffuser, increasing the flow rate may change the oscillating properties (e.g. the attenuation of “pulse force” due to the build up of boundary layer), and may also cause bubble coalescence, consequently weakening the efficiency of oscillator for microbubble creation. Therefore, the microbubble size may slightly increase when the flow rate increases, resulting in a reduction of $d_{B\text{NoFO}}/d_{B\text{FO}}$ ratio, which leads to the decline of K_La improvement efficiency ($I\%$). This phenomenon also indicates a view that using fluidic oscillator to enhance mass transfer has its limitations in terms of flow rate (or to be more accurate, flow rate over liquid volume ratio).

3.3. The Relationship between Mass Transfer Coefficient and Overall Mass Transfer Rate

Knowing the mass transfer coefficient K_La helps to indicate the capability of mass transfer, while knowing the mass transfer rate gives a straight view of e.g. how rapidly the CO_2 dissolve into liquid, which also helps to estimate the CO_2 capture efficiency.

The instantaneous mass transfer rate (V_{MTR}) is interpreted as the driving force multiplied by the mass transfer coefficient (K_La) [16], shown in Equation (9),

$$V_{MTR} = \frac{d[\text{CO}_2]}{dt} = K_La \left([\text{CO}_2]^* - [\text{CO}_2]_t \right), \quad (9)$$

where K_La is the mass transfer coefficient (min^{-1}), both $[\text{CO}_2]_t$ and $[\text{CO}_2]^*$ are instantaneous concentrations of CO_2 and its equilibrium concentration ($\text{mol}\cdot\text{L}^{-1}$), respectively. The average mass transfer rate (V'_{MTR}) for a certain dosing time period (t_d) can be fairly represented as

$$V'_{MTR} = \frac{\int_0^{t_d} V_{MTR} dt}{t_d} = \frac{\int_0^{t_d} K_La \left([\text{CO}_2]^* - [\text{CO}_2]_t \right) dt}{t_d}. \quad (10)$$

Assuming

$$[\text{CO}_2]_t = [\text{CO}_2]_0 + V'_{MTR}t, \quad (11)$$

by solving Equation (10) and Equation (11), it gives:

$$\begin{aligned}
 V'_{MTR} &= \frac{\int_0^{t_d} K_L a ([CO_2]^* - [CO_2]_0 - V'_{MTR} t) dt}{t_d} \\
 &= K_L a [CO_2]^* - K_L a [CO_2]_0 - K_L a V'_{MTR} \frac{t_d}{2}, \quad (12) \\
 \Rightarrow V'_{MTR} &= \frac{K_L a ([CO_2]^* - [CO_2]_0)}{\frac{K_L a t_d}{2} + 1}
 \end{aligned}$$

where $[CO_2]_0$ represents the initial CO_2 concentration ($mol \cdot L^{-1}$) for a selected time period.

The accuracy of Equation (12) was examined via **Figure 5** which plots the experimental values of average mass transfer rates versus the calculated values by using Equation (12). Compared with examined values, most of the data calculated by Equation (12) showed only less than 10% difference.

3.4. CO_2 Capture Efficiency for Microbubble Dosing and Fine-Bubble Dosing

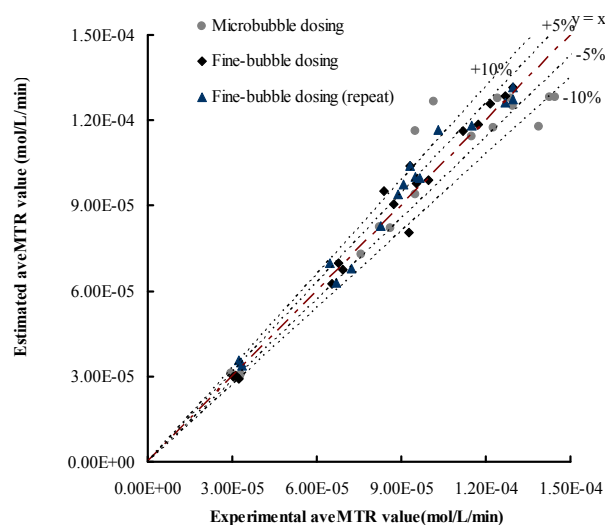
CO_2 capture efficiency is one of the most important parameter concerned by many bioprocesses with the purpose of CO_2 sequestration. Since the rate of CO_2 dissolving into liquid can be valued by overall mass transfer rate using Equation (12), the CO_2 capture efficiency (E_{CO_2}) can be therefore simply described as the amount of CO_2 been absorbed over the amount of CO_2 been fed into the liquid (m_s/m_d) within a specific dosing time period (t_d), shown in Equation (13).

$$E_{CO_2} = \frac{m_s}{m_d} = \frac{V'_{MTR} \times Vol \times t_d}{CO_2 \% \times V_F \times P / (RT) \times t_d} \quad (13)$$

where $CO_2\%$ means the percentage of CO_2 in the gas supply, Vol is the volume of the liquid (m^3), V_F is the gas dosing flow rate ($L \cdot min^{-1}$), P is standard atmosphere pressure (101,325 Pa), R is the ideal gas law constant ($8.314 J \cdot K^{-1} \cdot mol^{-1}$) and T is the temperature (298 K).

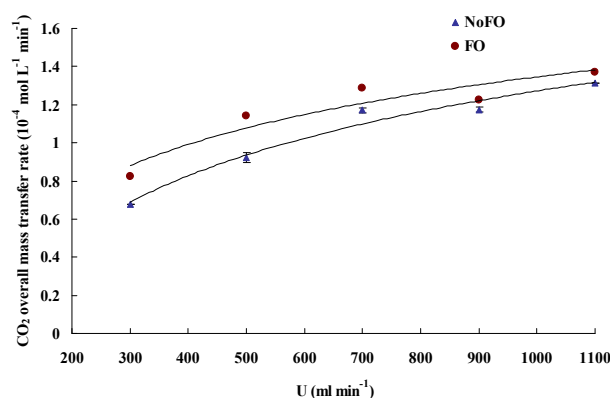
The CO_2 dissolving rate and the CO_2 capture efficiency under different dosing conditions were plotted in **Figures 6** and **7**, respectively. In general, micro-bubble dosing by using the fluidic oscillator was found to have both higher CO_2 dissolving rate (average mass transfer rate) and CO_2 sequestration efficiency for a wide range of dosing flow rate, but the level of improvements were attenuated as the flow rate went up (similar to the attenuation of $K_L a$ improvement, see 3.2). Such attenuation of improvement was caused by the increase in microbubble size due to the weakening of oscillation and bubble coalescence under higher flow rate.

Apart from reducing bubble size, increasing flow rate can also achieve a higher $K_L a$ (see 3.1), it is therefore not a surprise to found that the CO_2 overall mass transfer rate increases along with the flow rate (**Figure 6**). However,



The $K_L a$ value for each condition was obtained based on selected time period (5 - 10 min), via the standard method described by Chisti [16]. For each dosing condition, the average mass transfer rates for selected time period (5 - 8 min, 5 - 10 min and 5 - 12 min) were estimated by Equation (12) (Y-axis) and examined by $([CO_2]_t - [CO_2]_0)/t$ (X-axis).

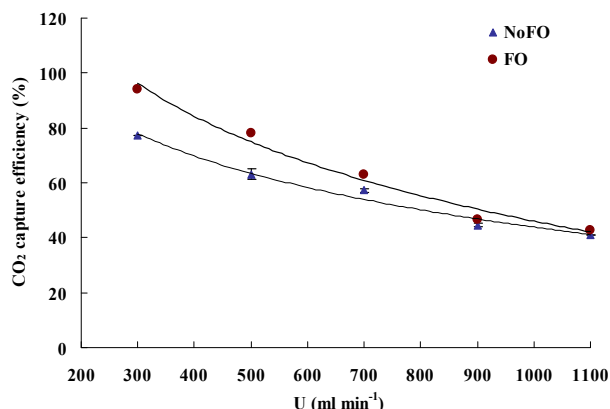
Figure 5. Plots of estimated average mass transfer rates versus examined values.



The average mass transfer rate was calculated based on Equation (12), and the time period selected for MTR' calculation under each dosing condition was between 5 min and 10 min after starting dosing, the same time interval used for the $K_L a$ estimation.

Figure 6. The average mass transfer rate under different dosing conditions.

it is interesting that the CO_2 capture efficiency actually reduces when the flow rate increases (**Figure 7**). Higher $K_L a$ dose mean higher CO_2 overall mass transfer rate (higher CO_2 dissolving rate), however, if the cost to achieve higher $K_L a$ is enhancing the dosing flow rate rather than reducing bubble size, then the amount of not dissolved CO_2 ("wasted CO_2 ") would increase, and such increase in wasted CO_2 could not be balanced by the increase in dissolved CO_2 , which ultimately lowers the CO_2 capture efficiency. Therefore, in order to achieve both higher CO_2 mass transfer rate and capture efficiency, reducing bubble size (e.g. using microbubbles) is more promising than increasing flow rate.



The CO₂ capture efficiency for each dosing condition was calculated based on Equation (13), and the time period selected for each calculation under different dosing conditions is the same as for overall mass transfer rate calculation.

Figure 7. The plots of CO₂ capture efficiency versus gas dosing flowrate.

3.5. Effect of NaHCO₃ on Equilibrium pH and CO₂ Mass Transfer Rate in Water

In microalgae culture, CO₂ is injected into the culture medium (usually containing NaHCO₃) rather than pure water. When adding NaHCO₃ into water, NaHCO₃ dissociates into sodium (Na⁺) and bicarbonate (HCO₃⁻) ions, and these HCO₃⁻ ions neutralize some of the H⁺ ions present in the medium to form the dissolved CO₂ and so increase the pH. So the concentration of NaHCO₃ clearly has an effect on pH, it is worth finding out whether the culture medium containing NaHCO₃ could affect the CO₂ mass transfer. Therefore, a separate experiment was carried out in a smaller version but the same design of airlift bioreactor (2.5 L).

Keeping other parameter constant (flow rate, temperature etc.), higher concentrations of NaHCO₃ added into distilled water should theoretically raise the minimal pH (equilibrium pH, pH*) reached after CO₂ dosing. According to Henry's law and Two-film theory, the equilibrium concentration of dissolved CO₂ ([CO₂]^{*}) should only depend on the CO₂ partial pressure in the gas phase for a fixed gas/liquid properties and temperature (assuming the changes in liquid physical properties by adding different amount of NaHCO₃ to the water, e.g. viscosity, are negligible, as long as the concentration of NaHCO₃ is low). Therefore, different concentrations of NaHCO₃ in the water should not affect the [CO₂]^{*}. On the other hand, the CO₂ concentration is correlated to pH by Equation (3). Since the concentration of Na⁺ varies for different concentration of NaHCO₃, while the [CO₂]^{*} does not change, it is therefore reasonable that pH* changes for the water containing various NaHCO₃ concentration. Indeed, this hypothesis was proved correct, in **Figure 8**, a log-linear trend was observed in the equilibrium pH values as the concentration of NaHCO₃ was increased. Besides, all the

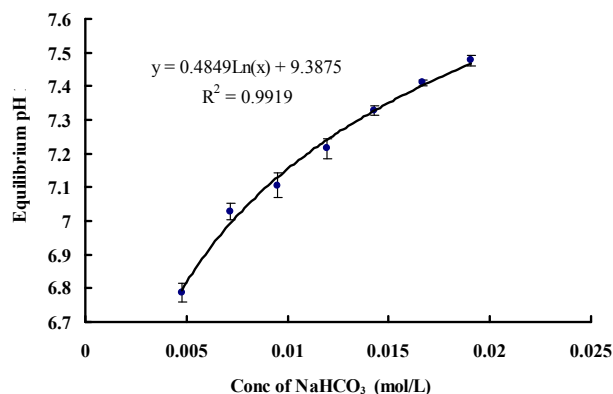


Figure 8. Change in equilibrium (final) pH for different concentration of NaHCO₃.

equilibrium concentrations of CO₂ corresponding to each equilibrium pH value under different concentrations of NaHCO₃ were found to be the same, which is approximately 0.0017 ± 0.0001 mol·L⁻¹. In terms of mass transfer for CO₂ dissolution, it can be seen that changing the concentration of NaHCO₃ does not have much of an effect on the mass transfer coefficient (**Figure 9**). Hence, NaHCO₃ could be used to control the equilibrium (minimal) pH of the medium without affecting the [CO₂]^{*} and *K_La*. The pH region can also be altered depending on the particular strain of microalgae being cultured, as different algae prefer different pH.

3.6. CO₂ Mass Transfer in Microalgae Culture

In order to test the effect of real microalgae culture on CO₂ mass transfer, 5% CO₂ was dosed into a healthy *D. Salina* culture (containing 0.012 mol/L of NaHCO₃) under a fixed flow rate (0.7 L/min) for 30 min, with pH recorded every 30 seconds. The results showed that there appears to be two distinct stages in terms of *K_La*, see **Figure 10** for example. The calculations leading to the determination of the *K_La* mass transfer coefficients from the slopes seen in **Figure 10** are given in **Table A1** (See Appendix).

From the calculations in **Table A1**, for the first 4.5 minutes of gas supply, the concentration of CO₂ dissolved and the resultant mass transfer is of different magnitudes when the pH is greater than 8.4. Once the pH is less than 8.4, the *K_La* is much higher in comparison. This was observed for each mass transfer test in culture medium with the threshold pH value of 8.4 seen each time. It is speculated that slower mass transfer at the start when pH is higher than 8.4 could be due to the chemical reactions taking place within the culture medium the gas is being bubbled through. Considering the dissociation of water into hydrogen (H⁺) and hydroxyl (OH⁻) ions, when the pH is over 8.4, the concentration of hydroxyl ions will be much greater than that of the hydrogen ions ($[OH^-] \ll [H^+]$). The [H⁺] produced when CO₂ dis-

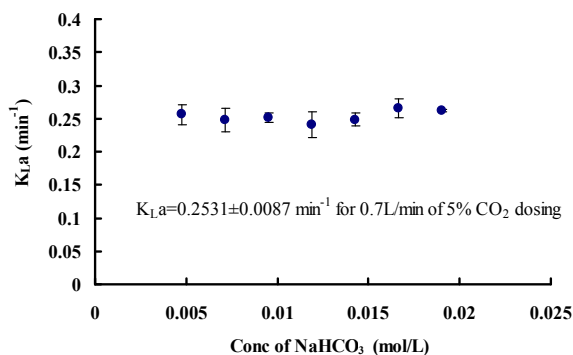
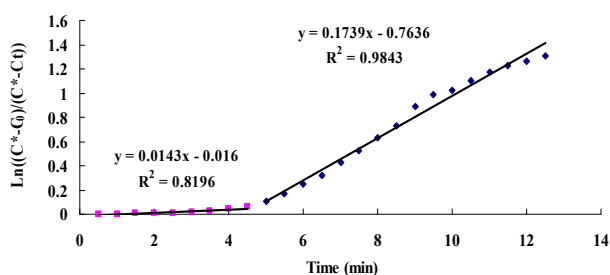


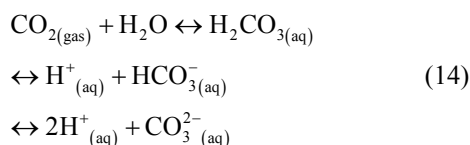
Figure 9. Changes in CO_2 mass transfer coefficients for different concentrations of NaHCO_3 .



The slope of straight line indicates mass transfer coefficient K_{La} (min^{-1}).

Figure 10. Typical plot for K_{La} estimation (for $0.7 \text{ L} \cdot \text{min}^{-1}$ dosing).

solves will be neutralized by $[\text{OH}^-]$ present in the medium. Considering the carbonate equilibrium system (Equation (14)) [18], this will result in less dissolved CO_2 and instead, more HCO_3^- . Hence, it is argued that the mass transfer for dissolved CO_2 will be low at relatively high pH as most of the supplied CO_2 will react to form the bicarbonate species rather than the desired dissolved CO_2 . At less alkaline pH values, this transfer will be less significant and dissolved CO_2 concentration will increase faster. This theory is also applicable to the mass transfer within a medium without microalgae, but such alkaline pH values were not encountered in the experiments conducted. Stemler (1980) also noted the effect of pH on the amount of dissolved CO_2 and discusses the effect of pH on the relative levels of CO_2 and HCO_3^- present within a solution [19]. He found that in going from pH 8.0 to 7.3, the amount of HCO_3^- changed very little while the concentration of CO_2 , on the other hand, increased more than 4-fold.



In total, the CO_2 mass transfer coefficient in the *D. salina* culture with $0.7 \text{ L} \cdot \text{min}^{-1}$ of 5% CO_2 gas dosing was found to be $0.0164 \pm 0.0046 \text{ min}^{-1}$ at $\text{pH} > 8.4$ and $0.1776 \pm 0.0064 \text{ min}^{-1}$ at $\text{pH} < 8.4$. For clarification pur-

pose, at $\text{pH} > 8.4$ the K_{La} for dissolved CO_2 is relatively low, but it does not mean less CO_2 from gas supply has been transferred into liquid. Actually, most of the CO_2 been transferred into culture was converted into HCO_3^- and CO_3^{2-} when $\text{pH} > 8.4$. Therefore, when calculating the CO_2 capture efficiency in future, the changes in the amount of total carbon (C_T) should be considered rather than the amount of dissolved CO_2 when $\text{pH} > 8.4$. But if the pH is less than 8.4, the changes in the amount of total carbon almost come from the changes in dissolved CO_2 , so it is fair to use the K_{La} of dissolved CO_2 for CO_2 capture efficiency estimation.

Comparing both CO_2 mass transfer (when $\text{pH} < 8.4$) under $0.7 \text{ L} \cdot \text{min}^{-1}$ of dosing for water containing NaHCO_3 and the culture medium including microalgae (with the same concentration of NaHCO_3), the K_{La} in water (0.2531 min^{-1}) was found to be greater than the one in the presence of *D. salina* (0.1776 min^{-1}). That may be because the cells in the medium increased its viscosity, which could have reduced the diffusivity of CO_2 from liquid film to liquid phase plus part of dissolved CO_2 could be consumed due to *D. salina* growth. Hence the rate of CO_2 diffusion into the culture was slowed down, whilst without *D. salina* present the CO_2 could diffuse much easier through the medium and without being consumed. Also, because of the changes in liquid properties, the CO_2 equilibrium concentration $[\text{CO}_2]^*$ was slightly smaller in the culture ($0.0011 \pm 0.0001 \text{ mol} \cdot \text{L}^{-1}$) than that in the NaHCO_3 medium ($0.0017 \pm 0.0001 \text{ mol} \cdot \text{L}^{-1}$).

4. Conclusions

For the same bubble generation method, enhancing the gas dosing flowrate can increase the mass transfer coefficient. For the same bubbling flowrate, reducing the bubble size can lead to an improvement on K_{La} as well. Compared with fine-bubble dosing, microbubbles dosing of 5% CO_2 gas by using fluidic oscillator has been proved to enhance the K_{La} for both CO_2 dissolution and O_2 removal by 30% - 100% across different flow rate. Despite K_{La} can be enhanced by either increasing the dosing flowrate (to be more accurate, flowrate/liquid volume ratio) or reducing the bubble size, increasing flow rate to achieve a higher K_{La} would also raise the amount of CO_2 being wasted (not dissolved) which would ultimately lower the CO_2 capture efficiency. Therefore, in order to achieve both higher CO_2 mass transfer rate and capture efficiency for the improvement of microalgal growth and CO_2 sequestration, reducing bubble size (e.g. using microbubbles) is more promising than increasing flow rate.

The K_{La} for CO_2 dissolution was not affected by the presence of NaHCO_3 , and NaHCO_3 could be used to control the equilibrium pH of the medium without af-

fecting the $[CO_2]^*$ and K_La . The pH region can also be altered depending on the particular strain of microalgae being cultured, as different algae prefer different pH. In the real algal culture, there appears to be two distinct stages in terms of K_La , divided by the pH of 8.4. When $pH < 8.4$, due to the changes in liquid properties and carbon system equilibrium relations, the K_La as well as $[CO_2]^*$ was found slightly reduced than the ones in the water.

Future works need to be done to test the effect of different percentage of CO_2 in the gas supply on mass transfer. And a mathematical model correlating mass transfer to bubble size, flow rate/liquid volume ratio and percentage of CO_2 in the gas supply etc. is expected to be established, which could facilitate the estimation of CO_2 dosing time for microalgae culture.

5. Acknowledgements

We acknowledge support for microbubble dynamics from EPSRC. WZ would like to thank the Royal Society for a Brain Mercer Innovation Award. DJG would like to acknowledge support from Carbon Trust.

REFERENCES

- [1] L. Xu, P. J. Weathers, X.-R. Xiong and C.-Z. Liu, "Microalgal Bioreactors: Challenges and Opportunities," *Engineering in Life Sciences*, Vol. 9, No. 3, 2009, pp. 178-189. [doi:10.1002/elsc.200800111](https://doi.org/10.1002/elsc.200800111)
- [2] A. Richmond, "CRC Handbook of Microalgal Mass Culture. Boca Raton," CRC Press, Florida, 1986.
- [3] A. P. Carvalho, L. A. Meireles and F. X. Malcata, "Microalgal Reactors: A Review of Enclosed Systems Design and Performance," *Biotechnology Progress*, Vol. 22, No. 6, 2006, pp. 1490-1506. [doi:10.1021/bp060065r](https://doi.org/10.1021/bp060065r)
- [4] A. Richmond, "Handbook of Microalgal Culture: Biotechnology and Applied Phycology," Wiley-Blackwell, New York, 2008.
- [5] O. Pulz, "Photobioreactors: Production Systems for Phototrophic Microorganisms," *Applied Microbiology and Biotechnology*, Vol. 57, No. 3, 2001, pp. 287-293. [doi:10.1007/s002530100702](https://doi.org/10.1007/s002530100702)
- [6] R. K. Gary, "The Concentration Dependence of the ΔS Term in the Gibbs Free Energy Function: Application to Reversible Reactions in Biochemistry," *Journal of Chemical Education*, Vol. 81, No. 11, 2004, pp. 1599-1604. [doi:10.1021/ed081p1599](https://doi.org/10.1021/ed081p1599)
- [7] A. P. Carvalho and F. X. Malcata, "Transfer of Carbon Dioxide within Cultures of Microalgae: Plain Bubbling Versus Hollow-Fiber Modules," *Biotechnology Progress*, Vol. 17, No. 2, 2001, pp. 265-272. [doi:10.1021/bp000157v](https://doi.org/10.1021/bp000157v)
- [8] D. R. Ketkar, R. Mallikarjunan and S. Venkatachalam, "Electroflotation of Quartz Fines," *International Journal of Mineral Processing*, Vol. 31, No. 1, 1991, pp. 127-138. [doi:10.1016/0301-7516\(91\)90009-8](https://doi.org/10.1016/0301-7516(91)90009-8)
- [9] J. K. Edzwald, J. P. Walsh, G. S. Kaminski and H. J. Dunn, "Flocculation and Air Requirements for Dissolved Air Flotation," *American Water Works Association*, Vol. 84, No. 3, 1992, pp. 92-100.
- [10] S. E. Rijk and J. G. Blanken, "Bubble Size in Flotation Thickening," *Water Research*, Vol. 28, No. 2, 1994, pp. 465-473. [doi:10.1016/0043-1354\(94\)90284-4](https://doi.org/10.1016/0043-1354(94)90284-4)
- [11] C. Tsouris, D. W. DePaoli, J. Q. Feng and T. C. Scott, "Experimental Investigation of Electrostatic Dispersion of Nonconductive Fluids into Conductive Fluids," *Industrial and Engineering Chemistry Research*, Vol. 34, No. 4, 1995, pp.1394-1403. [doi:10.1021/ie00043a047](https://doi.org/10.1021/ie00043a047)
- [12] L. A. Féris and J. Rubio, "Dissolved Air Flotation (DAF) Performance at Low Saturation Pressures," *Filtration & separation*, Vol. 36, No. 9, 1999, pp. 61-65. [doi:10.1016/S0015-1882\(99\)80223-7](https://doi.org/10.1016/S0015-1882(99)80223-7)
- [13] W. B. Zimmerman, V. Tesar, S. Butler and H. C. H. Bandulasena, "Microbubble Generation," *Recent Patents on Engineering*, Vol. 2, No. 1, 2008, pp. 1-8. [doi:10.2174/187221208783478598](https://doi.org/10.2174/187221208783478598)
- [14] W. B. Zimmerman, B. N. Hewakanadamby, V. Tesar, H. C. H. Bandulasena and O. A. Omotowa, "On the Design and Simulation of Airlift Loop Bioreactor with Microbubble Generation by Fluidic Oscillation," *Food and Bioprocess Processing*, Vol. 87, No. 10, 2009, pp. 215-227. [doi:10.1016/j.fbp.2009.03.006](https://doi.org/10.1016/j.fbp.2009.03.006)
- [15] W. B. Zimmerman, M. Zandi, H. C. H. Bandulasena, V. Tesar, D. J. Gilmour and K. Ying, "Design of an Airlift Loop Bioreactor and Pilot Scales Studies with Fluidic Oscillator Induced Microbubbles for Growth of a Microalgae *Dunaliella salina*," *Applied Energy*, Vol. 88, No. 10, 2011, pp. 3357-3369. [doi:10.1016/j.fbp.2009.03.006](https://doi.org/10.1016/j.fbp.2009.03.006)
- [16] M. Y. Chisti, "Airlift Bioreactors," Elsevier Applied Science, London, 1989.
- [17] K. Ying, D. J. Gilmour, Y. Shi and W. B. Zimmerman, "Growth Enhancement of *Dunaliella salina* by Microbubble Induced Airlift Loop Bioreactor (ALB)—The Relation between Mass Transfer and Growth Rate," *Journal of Biomaterials and Nanobiotechnology*, No. 4, 2013, pp. 1-9. [doi:10.4236/jbnb.2013.42A001](https://doi.org/10.4236/jbnb.2013.42A001)
- [18] R. Corfield, "The Carbon Cycle," In: C. Cockell, Ed., *An Introduction to the Earth-Life System*, Cambridge University Press, Cambridge, 2008, pp. 61-93.
- [19] A. Stemler, "Forms of Dissolved Carbon Dioxide Required for Photosystem II Activity in Chloroplast Membranes," *Plant Physiology*, Vol. 65, No. 6, 1980, pp. 1160-1165. [doi:10.1104/pp.65.6.1160](https://doi.org/10.1104/pp.65.6.1160)

Appendix

Table A1. An example of calculations leading to the CO₂ mass transfer coefficient (for 0.7 L·min⁻¹ dosing)

Time (s)	pH	[CO ₂] (Equation (3)) (mg·L ⁻¹)	$\ln([\text{CO}_2]^* - [\text{CO}_2]_0)/([\text{CO}_2]^* - [\text{CO}_2]_t)$	$K_L a$ (min ⁻¹)
0	9.554	6.13E - 06	N/A	
0.5	9.498	7.17E - 06	0.0010	
1	9.418	8.94E - 06	0.0026	
1.5	9.332	1.13E - 05	0.0047	
2	9.244	1.42E - 05	0.0074	0.0143
2.5	9.131	1.90E - 05	0.0118	
3	9.034	2.42E - 05	0.0167	
3.5	8.898	3.39E - 05	0.0257	
4	8.725	5.16E - 05	0.0424	
4.5	8.565	7.56E - 05	0.0656	
5	8.37	1.20E - 04	0.1097	
5.5	8.208	1.75E - 04	0.1677	
6	8.056	2.49E - 04	0.2515	
6.5	7.969	3.05E - 04	0.3195	
7	7.869	3.85E - 04	0.4252	
7.5	7.801	4.51E - 04	0.5217	0.1739
8	7.741	5.18E - 04	0.6310	
8.5	7.699	5.71E - 04	0.7264	
9	7.643	6.50E - 04	0.8882	
9.5	7.616	6.92E - 04	0.9860	
10	7.606	7.08E - 04	1.0265	